The Resistivity Log and Its Role in Understanding Sediment Unloading in the Lower Kutai Basin, Indonesia

STEPHEN O'CONNOR[1], AGUS M. RAMDHAN[2], ARIFIN[2,3], and AMY C. ELLIS[4]

[1]Global Geopressure Advice, Durham, UK
[2]Department of Geology and Department of Groundwater Engineering, Institut Teknologi Bandung, Bandung, Indonesia
[3]Department of Geography, University College London, London, UK
[4]AE Geosciences, Bristol, UK; currently at bp, London, UK

Corresponding author: agusmr@itb.ac.id
Manuscript received: May, 11, 2023; revised: July, 25, 2023;
approved: August, 10, 2023; available online: November, 17, 2023

Abstract – High overpressure is a critical drilling issue in the Lower Kutai Basin. Typical pore pressure prediction approaches involve an empirical relationship, such as Eaton's method using sonic log data. In areas with high geothermal gradients, such as the Lower Kutai Basin, there is evidence for additional overpressure from gas generation such that sediment unloading must be considered to interpret pore pressure correctly. In this paper a repeatable deterministic model is presented for pore pressure from sonic data and, using selected wells from the Lower Kutai Basin, also the use of the resistivity log in a similar model. In the Lower Kutai Basin, sonic logs are often absent from the logging suite or otherwise running over limited intervals, making an alternative log-based prediction method particularly valuable. As a caveat, shallow freshwater encroachment is reported in the Lower Kutai Basin, means the shallow resistivity data can be problematic to use to define both top of overpressure and a normal compaction trend. Care must therefore be taken if resistivity is to be used for the interpretation of unloaded pore pressure, and chiefly applied and this likely to be more successful where encroachment is less pronounced, such as pro-delta shales. Assuming the additional care needed in using resistivity data, this paper suggests that resistivity can be a useful tool for pore pressure prediction in unloaded shale at elevated temperatures within the Lower Kutai Basin. At present the technique has been applied to only a limited dataset due to data availability limitations, but it is hoped with further refinement it will form a helpful additional approach in the pore pressure prediction toolkit.

Keywords: pore pressure, resistivity, unloading, Lower Kutai Basin

INTRODUCTION

Significant overpressure, that is the differential pressure between *in-situ* and hydrostatic pressure, is documented in The Indonesia Neogene Lower Kutai shelfal areas in such wells as B-11 at Bekapai Field and onshore in SEM-39 at Semberah Field (Figure 1). Most wells in the shelfal area only penetrated down to the transition zone to hard overpressure (Ramdhan and Goulty, 2010). Pore pressures in the shelfal area have a sharp transition zone, within 1,000 ft. of the top of overpressure, and some wells have reached the hard overpressure zone where pore pressures are
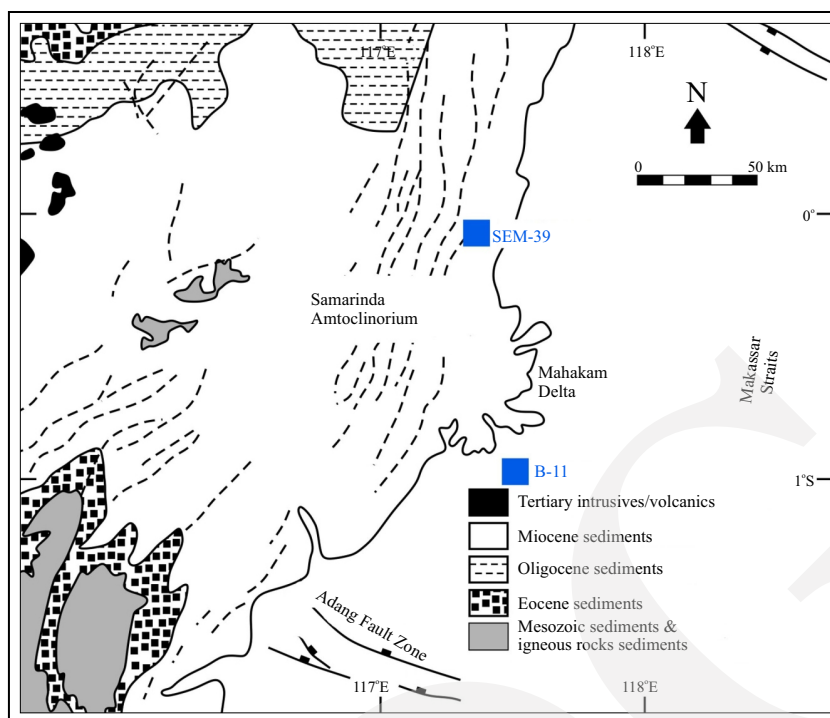
Figure 1. Simplified geological map of the Lower Kutai Basin showing the location of two wells analyzed in this study, B-11, and SEM-39 (modified from Chambers *et al.*, 2004).

close to the overburden or vertical stress. Well B-11, as an example, was drilled through the short transition zone at Bekapai Field, and the mud-weight was increased by approximately 2.1 ppg at depth increments of 300 ft. On the other hand, in the Semberah Field onshore, overpressure is characterized by a long transition zone into hard overpressure (Apranda *et al.*, 2019).

The cause of the hard overpressure in the Lower Kutai Basin has been attributed by previous studies to disequilibrium compaction associated with rapid burial (*e.g.* Bois *et al.*,1994; Bates, 1996; Burrus, 1998). However, more recent studies have reappraised these analyses, and noted resistivity and sonic logs display reversals in the transition zone into hard overpressure. Yet, the density log keeps increasing below the top of overpressure despite the vertical effective stress decreasing monotonically (Ramdhan and Goulty, 2010, 2011). Applying the Equivalent Depth Method, an approach based on an assumption of disequilibrium compaction, would result in under-prediction of deep overpressure. Pressure analysis in basins with high geothermal gradients and

based on the disequilibrium compaction concept can lead to underestimation of overpressure by as much as 20 MPa, compared to measurements in adjacent sands (Ramdhan *et al.*, 2011). Further analysis shows that clay diagenesis and gas generation, mostly temperature-driven, are essential in generating overpressure in the basin. Other authors, such as Ginanjar *et al.* (2015), similarly propose secondary mechanisms of overpressure for the Lower Kutai Basin, identifying four main geopressure zones vertically - normal hydrostatic pressure, abnormal pressure due to disequilibrium compaction, clay mineral transformation, and in the deeper section, by hydrocarbon generation.

In terms of indirect overpressure prediction in the Lower Kutai Basin, an approach using anomalous porosity such as Eaton (1975), and indeed, Equivalent Depth Method, is frequently unsuccessful in interpreting overpressure magnitude correctly, especially in hot mudrocks acted as source rocks or have experienced chemical changes. These additionally increase pore pressure via unloading. These typical mudrocks can be found in the Lower Kutai Basin (Ramdhan

and Goulty, 2010). Hence, it is very challenging to develop a general workflow for estimating the overpressure magnitude in this basin using a relationship that includes empirical constants. This paper highlights a deterministic approach discussed in a recent paper by Ramdhan and O'Connor (2022), developed based on sonic data. The deterministic model is applicable in estimating overpressure generated by loading, unloading, or both. The method was developed after the works of Ramdhan and Goulty (2018), with a simpler and easier way of use.

In addition, an often-ignored potential approach to investigate sediment unloading is to use the resistivity log. The resistivity log has been extensively applied qualitatively in correlating formations penetrated as well as providing indications of reservoir content, typically the presence of hydrocarbons and conductivity of connate or formation waters (Archie, 1942). It also has utility in interpreting pore pressure, and is commonly used for this purpose, more often in association with Eaton (1975), where disequilibrium compaction is present. The hypothesis tested here is based on observations by Hermanrud *et al.* (1998) where log responses in the intra-Jurassic shales, Norway, revealed that neutron and density logs do not show a significant difference in porosity between shales that are low vs. high in overpressure, whereas the sonic and resistivity responses show higher (apparent) porosity differences. It is suggested that the porosity is unaffected by differences in pore pressures, but that the sonic and resistivity logs are reacting to textural changes induced in the shales by overpressure rather than high porosities due to undercompaction. The authors explain these phenomena as sonic and resistivity logs measuring the transport properties of the rocks, *i.e.* interconnecting pores. Whereas the neutron and density measure bulk rock properties such as bulk porosity. As the resistivity log measures a rock ability to transmit electrical signals, improved connectivity in the water phase via overpressure would result in low resistivity and higher log porosity. The early work by Mann and Mackenzie (1990) attributed the presence of overpressure in

these formations to compaction disequilibrium as the overpressure generating mechanism. Although other theories have been presented to explain the high overpressures in Norway (42 MPa in the Kristin Field, for example: lateral transfer: Vik *et al.* (1992), Nysæther (2006) or quartz cementation, Bjørkum and Nadeau (1998), the consensus in the shales is for some factors of secondary processes such as elastic or inelastic unloading, *e.g.* Teige *et al.* (1999).

Bowers (2002) showed a high-pressure well, Cotton Valley, where sonic and resistivity logs showed clear reversals, whereas the density log did not. Modeled pore pressures are underestimated compared to mud weights used during the drilling, and the direct pore pressure data (RFT's). Bulk properties versus transport properties were cited. According to Bowers and Katsube (2002), sonic velocity and resistivity generally experience a more elastic rebound compared to bulk density and porosity. While bulk properties depend only on the net volume of the pore, transport properties are more sensitive to the shape and size of pores and how they are interconnected.

As it seems that the resistivity log is also reacting to overpressure in these published studies by Hermanrud *et al.* (1998) and Bowers (2001), it is proposed in this paper that resistivity data could be utilized in a similar way to sonic data to produce an approach to interpret pore pressure when unloading is present. This has not been previously investigated and published. Whilst the resistivity log is typically affected by more borehole corrections, including temperature and concerns about salinity variation, and so using sonic is preferable, many of the wells in the Lower Kutai Basin do not have sonic logs or, if present, they are over limited depth intervals. Thus, the use of the resistivity log may prove to be a useful tool to determine unloading in this basin, and others.

Geologic Overview

The Lower Kutai Basin was formed during an extensional phase that took place from Late Oligocene to Early Miocene (Moss and Chambers, 1999; Chambers *et al.*, 2004). The deposition of

syn-rift sediments in the Lower Kutai Basin took place after rifting from Middle to Late Eocene. Subsequently, shale-dominant deep marine sediments were deposited in the basin centre during Late Eocene to Late Oligocene. Deltaic sedimentation in this basin started from Early Miocene, and still continues offshore to the present day. Figure 2a shows the simplified stratigraphic column for this basin.

Bekapai Field

The Bekapai Field, a giant oil and gas field in the Lower Kutai Basin, has a faulted anticline structure (DeMatharel *et al*., 1980) with approximately north-south main fault orientation, dividing the field into three compartments. Production has been known from the west compartment only. The upper part of the Fresh Water Sand (FWS) unit, deposited in Late Miocene, is the largest contributor to oil production from this field. Meanwhile, the productive gas zones are the Pliocene Shallow Reservoir Zone and the underlying Late Miocene Tunu Main Zone. The rate of sedimentation of Bekapai

Field, represented by B-11, has been constant since Middle Miocene, with an average of more than 300 m Ma^{-1} (Figure 2b). In the west compartment, the top of overpressure is encountered at depths ranging from 3 to 3.5 km below sea level, where temperatures range from 120 – 135°C (Ramdhan and Goulty, 2018), as indicated in Figure 2d. An analysis using a pressure-depth plot as well as wireline log responses of an overpressured well in the Bekapai Field indicates that in this field, the overpressure can be close to the vertical stress (Ramdhan and Goulty, 2014).

Semberah Field

This field was discovered in 1974, and field reservoirs consist of many layers of delta plain and delta front deposits. These lie within a two-way structural trap and are bounded by a thrust fault to the west. The hydrocarbon accumulation is distributed both vertically and laterally within Balikpapan Formation, Middle Miocene age, with reservoirs intercalating between delta plain and delta front facies (Riadi *et al*., 2018). This forma-
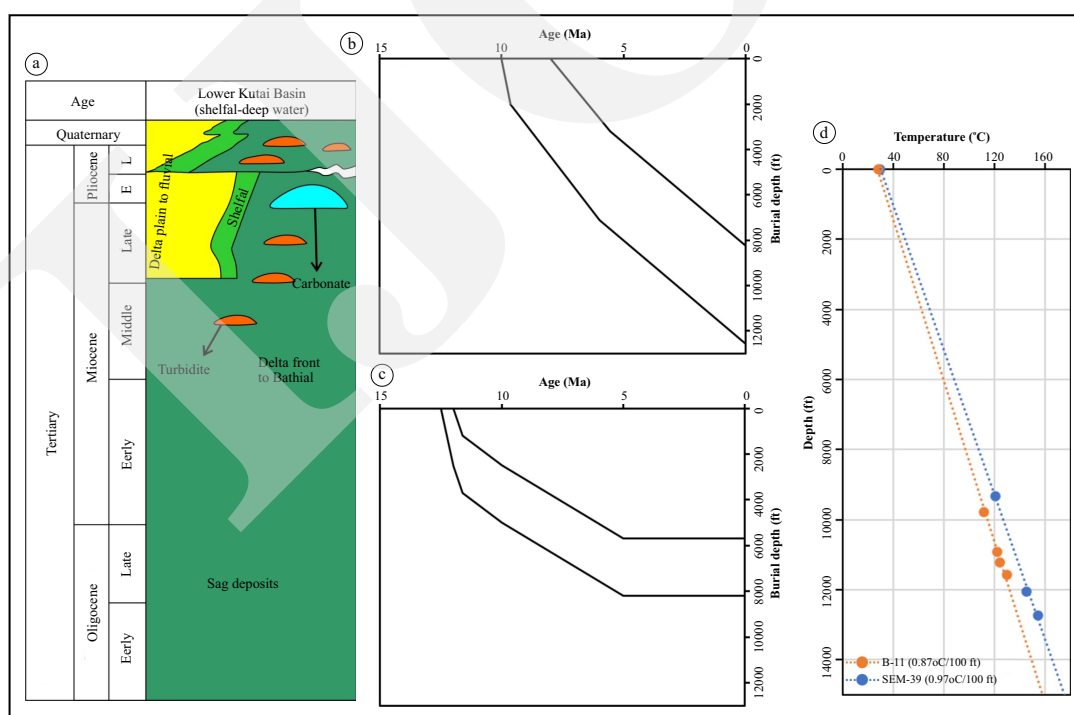

Figure 2. From left a) The simplified stratigraphic column of the Lower Kutai Basin (modified from Chambers *et al*., 2004). b) The typical burial history of B-11. c) The typical burial history of SEM-39, taken from a nearby offset well. d) The plot of temperature against depth, showing the thermal gradient in both wells. Blue temperature data (SEM-39) are from RFT, while the orange data (B-11) are BHT corrected using Horner and DST.

tion presents a challenging reservoir characterization with its interposing sandstone-claystone, and discontinuous reservoir enclosed by coal layer as the top of flooding surfaces. The stratigraphic interpretation of the formation uses a maximum flooding surface correlation with discernible thick shale sediment between the coal layers (Widyantoro and Santoso, 2021). Post-production wells drilled in the northern part of the I Zone thick channel sand experience pressure of ~ 7.5 to 8 ppg in areas C and D, compared to A and B which range from ~ 1.5 to ~4.5 ppg, indicating C and D are isolated reservoirs which are not connected to other reservoirs. The Semberah Field is more isolated due to significant marine influence (Riadi *et al.*, 2018). No sedimentations have taken place in this field since approximately Pliocene due to erosion, as illustrated in Figure 2c.

METHODS

In order to justify the use of the approach described by Ramdhan and O'Connor (2022), first, it is necessary to determine which mechanisms of overpressure generation are present. As previously mentioned, disequilibrium compaction relates to anomalously high porosity. Whereas in unloaded sediments, such porosity anomaly will not be found. Developing a cross-plot of sonic and density logs is a simple but very useful way to identify the overpressure-generating mechanism. As illustrated in Figure 3, Dutta (2002) and Katahara (2006) developed a cross-plot with two compaction lines, smectitic and illitic lines corresponding to linear equations. The smectitic and illitic lines correspond to the upper and lower bounds developed by Gardner *et al.* (1974) and Bowers (1995), respectively. Bowers (2001) suggested an alternative of which axes should represent which wireline log. If the density log is available, the cross-plot can indicate whether unloading acts as the overpressure generating mechanism, *i.e.* when the density log fails to follow the expected pattern of the sonic log when only loading contributes to the overpressure,
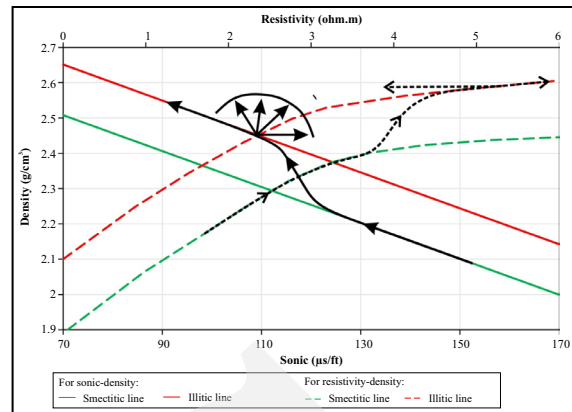

Figure 3. Cross-plot of sonic-density (Dutta, 2002; Katahara, 2006) and resistivity-density showing the smectitic and illitic trends.

and potentially, the causative mechanisms. After successfully determining whether only loading or both loading and unloading is present, the appropriate pore pressure estimation algorithm can be chosen (*e.g.* Eaton, 1975; Bowers, 1995).

As a test of the hypothesis of Hermanrud *et al*. (1998), and, by implication, Bowers (2001), the resistivity log should react in a similar manner to the sonic log, that is, a response to sediment unloading. This paper focuses primarily on two wells, B-11 in the Bekapai Field and SEM-39 in the Semberah Field. Each of these wells features a full well suite as well as Wireline Formation Tests, *e.g.* Repeat Formation Tests.

The vertical stress is calculated using the following equation:

$$\sigma_v = \int_0^z \rho_b g dz \quad \text{... (1)}$$

where:
σ_v= vertical or overburden or lithostatic stress
z= depth
ρ_b= bulk density represented by the density log
g = gravitational acceleration
For the B-11 well, $\sigma_v = 0.2263 * z^{1.1538181}$, while for the SEM-39 well, $\sigma_v = 0.4746 * z^{1.0828342}$.

When overpressure is generated by loading, the velocity (the reciprocal of transit time of sonic log) and effective stress can be related using Equation 2 (Bowers, 1995). As can be implied, Equation 2

indicates that mudrocks with the same velocity also have the same effective stress. Therefore, the pore pressure can later be calculated by subtracting the effective stress calculated from Equation 2 from the vertical or overburden stress.

$$\sigma_L' = \frac{VL - 5000^{1/b}}{a} \quad .... (2)$$

where:

σ_L' = effective stress when overpressure generated only by loading

V_L = velocity for overpressure generated by loading or V_{max}

a and b are constants calibrated with offset velocity-effective stress data

5000 represents the sonic velocity of seawater in ft/s

In the work by Ramdhan and O'Connor (2022) for the Lower Kutai Basin, a = 7.5452 and b = 0.8137. Based on Gulf Coast data, an additional equation was presented by Bowers (1995) regarding the overpressure generated by unloading, specifically by fluid expansion (Equation 3). Even though velocity reversals found in the Lower Kutai Basin coincide with the gas generation, the causative mechanism of the unloading was not speculated.

$$\sigma_T' = \sigma_L' \left(\frac{V - 5000}{VL - 5000} \right)^U \quad .... (3)$$

where:

σ'_T = total effective stress owing to loading and unloading

V = velocity data

U = unloading constant or parameter

A U value of 4.5 was used in Ramdhan and O'Connor (2022) for the Lower Kutai Basin. Those a and b values were used and determined for B-11 in the above paper to interpret pore pressure in a new well, SEM-39, Semberah Field. In this well, a model using resistivity data was constructed to identify loading and unloading. Then as a test, this model was re-applied to B-11.

Due to the absence of significant lithological change, it is assumed that mudrocks in The Lower Kutai Basin are similar. The Vmax is set as the velocity of the mudrocks at the very first point of the reversal, representing the highest effective stress. The unloading constant (U) indicates the plasticity of the mudrocks. When U=1, it indicates elastic deformation or no permanent deformation. This was assumed by Eaton (1975) as well as Hottman and Johnson (1965). A U value of infinity represents plastic deformation (irreversible deformation). Practically, U ranges in value between 3 and 8 (Bowers, 1995).

As no a and b values presently exist using resistivity data for The Lower Kutai Basin, in this paper, a similar approach to sonic was used, in that, vertical effective stress was plotted against shale velocity for each of any relevant Wireline Formation Tests. The shale velocity was determined using the resistivity log, and looking for a consistent response, either above or below the particular test in question. A window of 20 m was applied, where possible, to determine an average resistivity for the velocity/stress model. For data that plot in a different resistivity/stress space, and assumed unloaded, a separate pressure/stress trend was determined. These models were interchanged at the depth at which the unloading is considered active and based on the illitic line in Figures 4 and 5 (left-hand side: sonic), and on the deviation on the resistivity/density plots (Figures 6 and 7; right-hand side).

RESULT

The cross-plots of density and sonic in Figures 4 and 5 show observable shifts to velocity reduction, followed by densities of ~2.5 g cm^{-3} or higher in the analyzed wells. The high densities do not comply with disequilibrium compaction, thus, indicating chemical compaction, *i.e.* smectite–illite transformation. The reversal in velocity indicates the presence of unloading, even though the muted density reversal indicates disequilibrium compac-
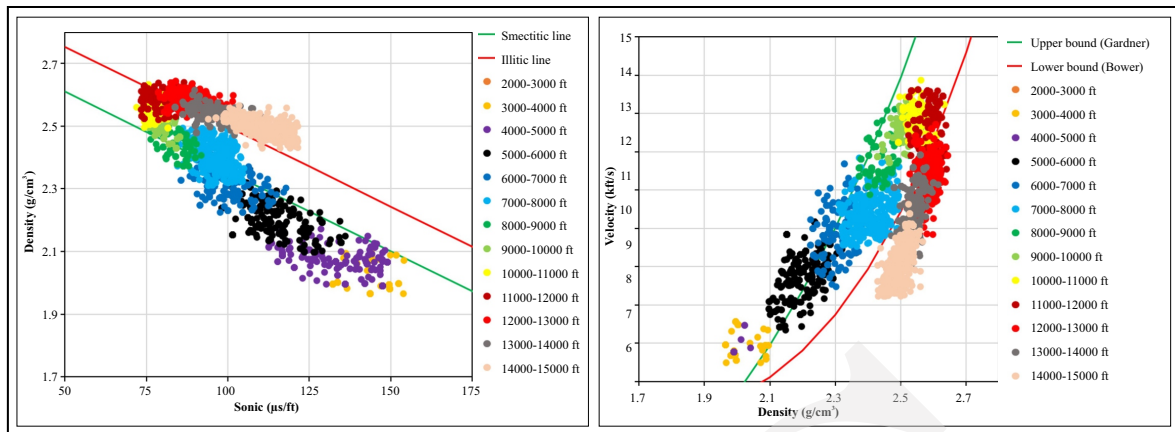
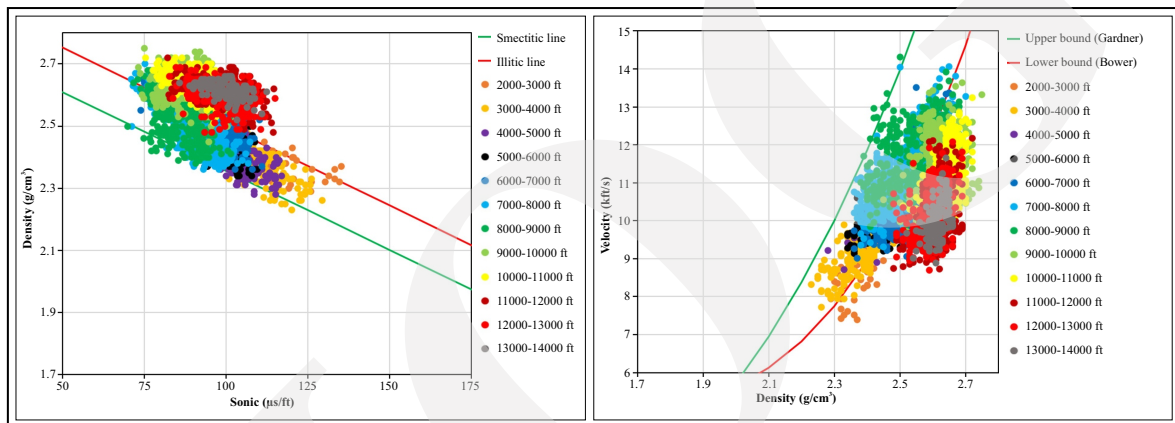Figure 4. Cross-plots of sonic-density (left) and density-velocity (right) for B-11.

Figure 5. Cross-plots of sonic-density (left) and density-velocity (right) for SEM-39.
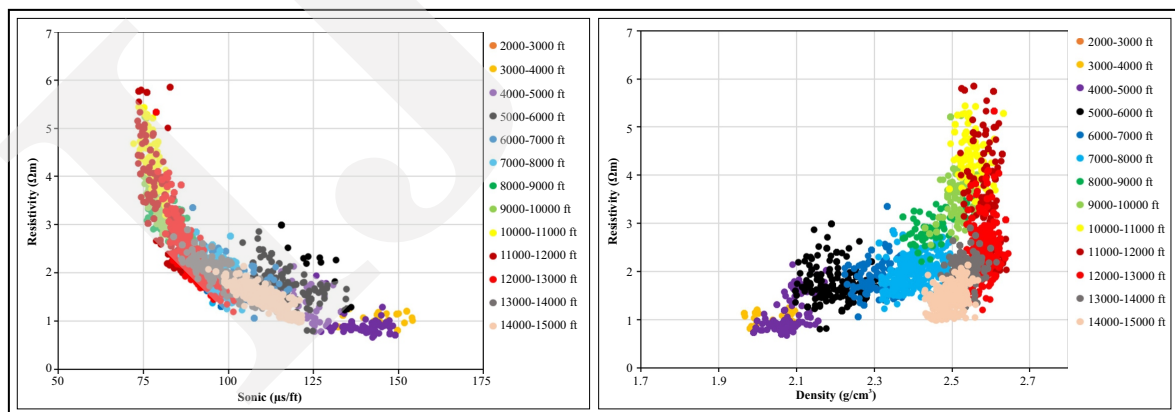

Figure 6. Cross-plots of sonic-resistivity (left) and density-resistivity (right) for B-11.

tion that also has some contribution. Shale/sands in the wells analyzed are highly overpressured, as indicated by the direct pressure data, which shows the overpressures are close to lithostatic (Figures 8 and 9).

In Figures 6 and 7, similar cross-plots are displayed, based on Dutta (2002) and Katahara (2006). However, here, comparing resistivity and density. On the left-hand side of each, the sonic and resistivity present as a consistent trend, or
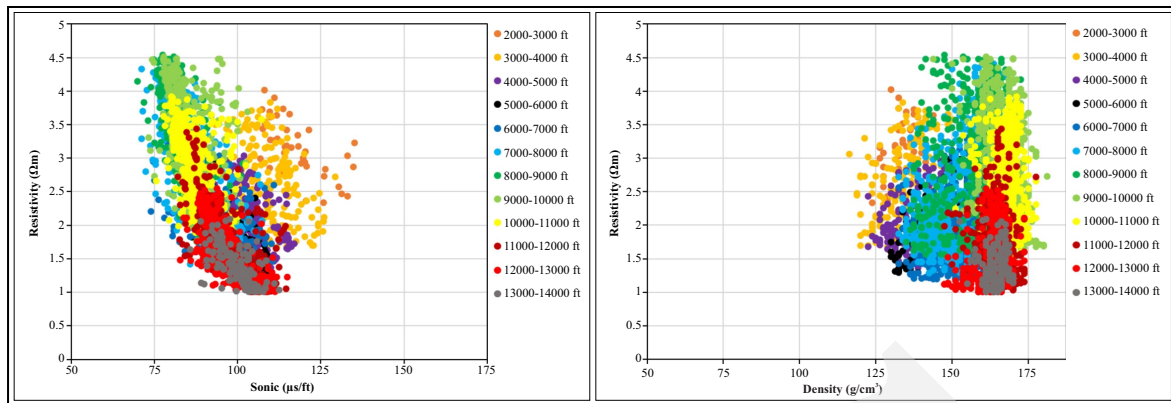
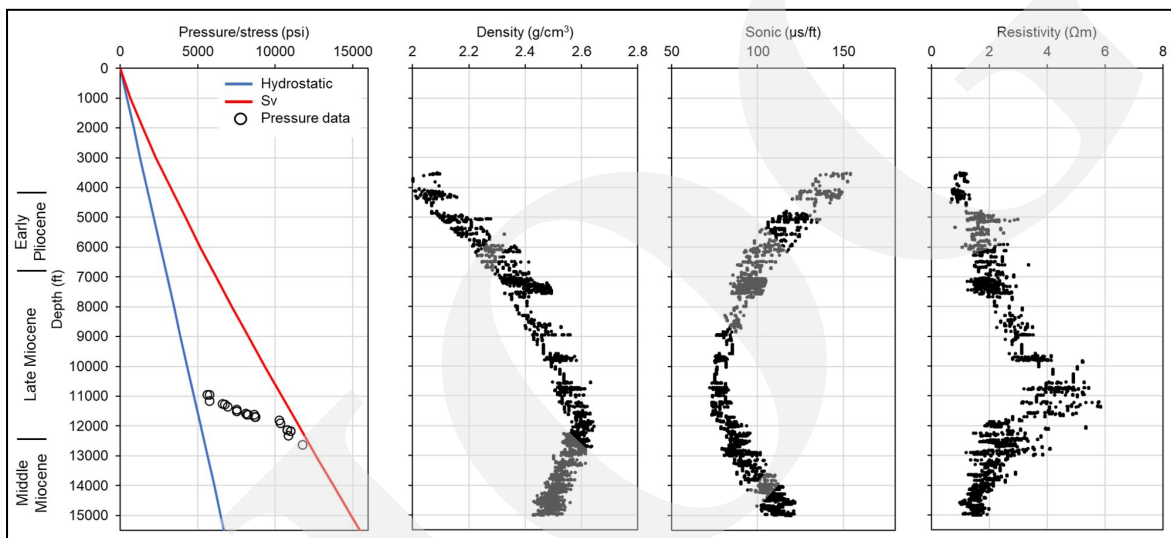Figure 7. Cross-plots of sonic-resistivity (left) and density-resistivity (right) for SEM-39.

Figure 8. Pressure data and wireline logs in the shale section of B-11.
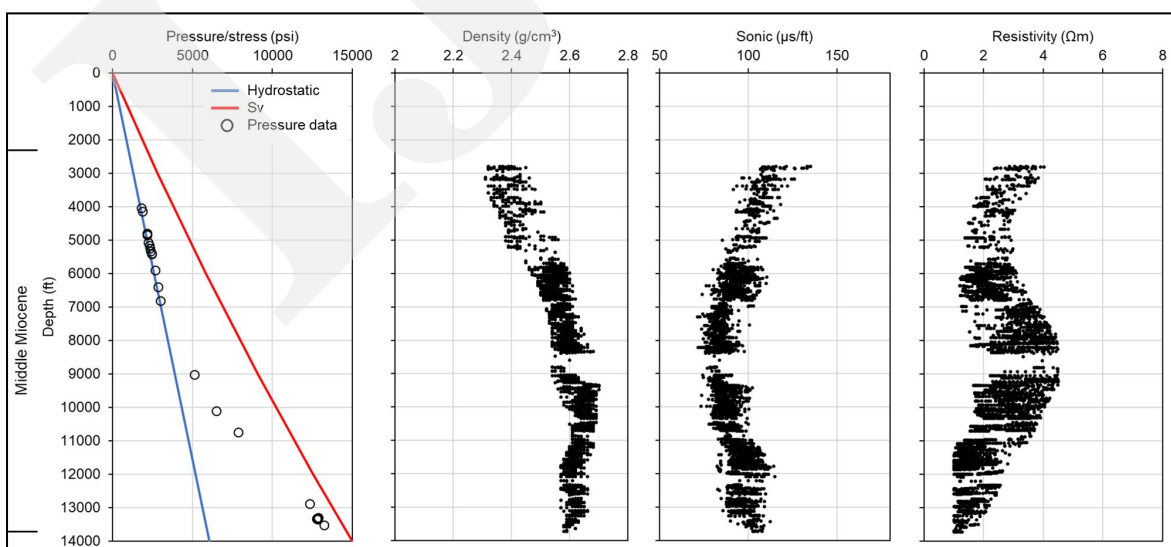

Figure 9. Pressure data and wireline logs in the shale section of SEM-39. Note that the stratigraphic marker was obtained from a close neighbour well.

rather, show a sympathetic relationship, expected if both logs were responding to pore pressure and stress in the same way. On the right-hand side, like sonic and density, resistivity deviates in shales of elevated temperatures.

As mentioned previously, in the work by Ramdhan and O'Connor (2022), for the Lower Kutai Basin, a = 7.5452 and b = 0.8137. These parameters were derived using data from the B-11 well, and here these have been taken and applied to the new well, SEM-39. These parameters and Equation 2 have been integrated to produce pore pressure interpretation for both wells. Figure 10 in green are the pore pressures assumed to represent generated by disequilibrium compaction alone. These substantially under-estimate the measured (undrained) reservoir pressures, particularly in the hotter intervals of both wells. Therefore, an unloading constant (U) of 4.5 (derived from B-11, Ramdhan and O'Connor, 2022) was used for Equation (3) to match the measured pore pressures in the new well. Ramdhan and Goulty (2010, 2011) suggested the kerogen-gas transformation as the mechanism responsible for the unloading. Although the overpressure is mainly generated

by unloading due to gas generation, loading contributed first to the overpressure occurrence within the pro-delta mudrock-dominated sequence. The onset of gas generation can be found within the transition from the delta front into the pro-delta sequence. Figure 10 also shows the pore pressure interpretation for unloading in red, now matching the reservoir measured pressures.

As well as seeing if the a and b values determined in Ramdhan and O'Connor (2022) are transferable to other Lower Kutai Basin wells, the resistivity was also used to detect the presence of unloading. Thus, the log as an additional method was used in calculating the pore pressure in the absence of a sonic log. Figure 11 (upper) shows the results of cross-plotting resistivity and vertical effective stress for the repeat formation tests. Those tests, representative of cooler shales, define a concave trend, in contrast to the typical convex shape observed when using sonic data and as observed in Bowers (1995).

To simplify the mathematics, the x and y-axes were reserved in Figure 11 (lower) to produce a loading (Equation 4) and an unloading curve (Equation 5):
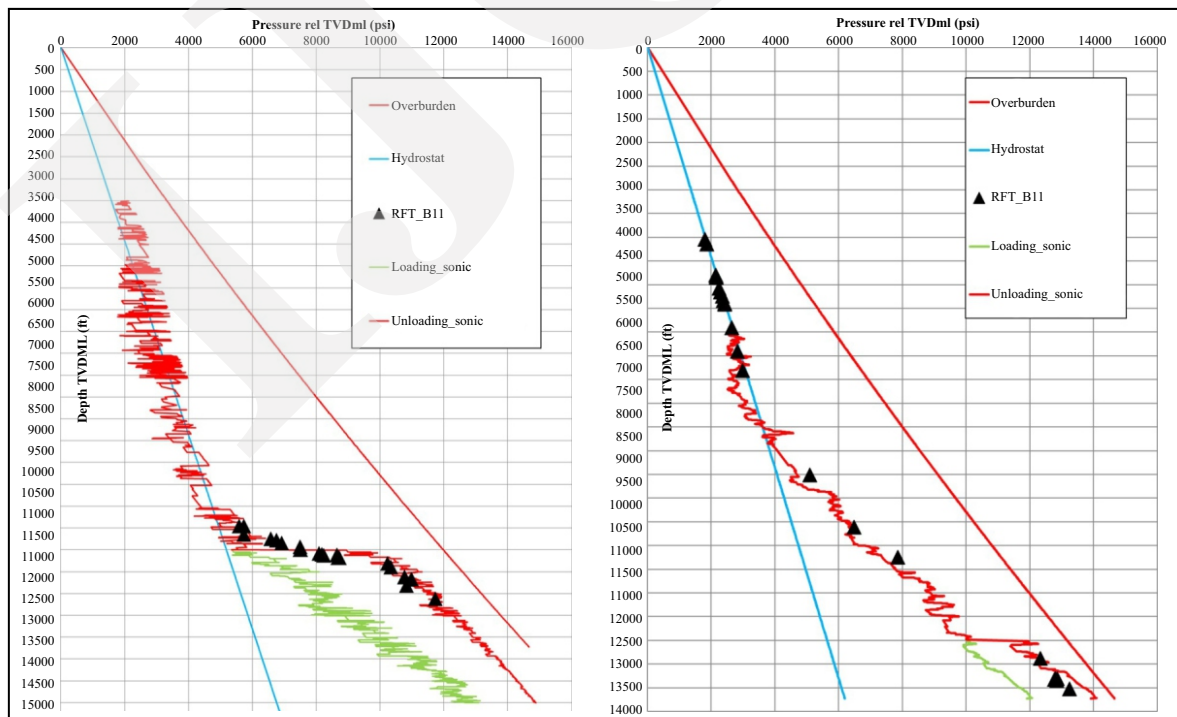

Figure 10. Result of pore pressure estimation using sonic data in B-11 (left) and SEM-39 (right).
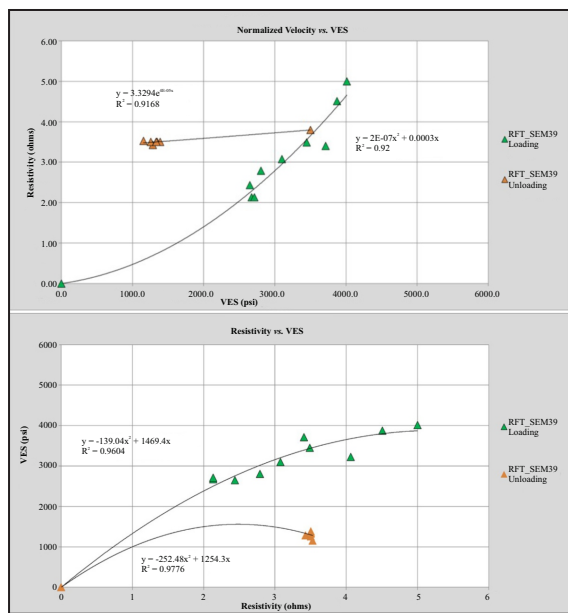
Figure 11. Cross-plots between resistivity and vertical effective stress. Upper figure plots the data following Bowers (1995). Lower figure re-plots the same data by switching axes to allow mathematical solvability.

$$\sigma_{Lr}' = -139.04 * r^2 + 1469.4 * r \quad .... (4)$$

where:

σ_{Lr}' = predicted effective stress resulting from loading

r = resistivity log value (ohmm)

and:

$$\sigma_{Lru}' = -252.48 * r^2 + 1254.3 * r \quad .... (5)$$

where:

σ_{Lru}' = predicted effective stress for overpressure generated by unloading

In Figure 12, pore pressure interpretation (based on resistivity) for loading is in green, and for unloading is in red.

DISCUSSION

Ideally, a sonic log is the preferred dataset to determine the contribution of loading and unloading in the Lower Kutai Basin. Reasons for this include the inherent nature of the resistivity log, such as requiring temperature correction and accounting for variation in salinity. Other factors include borehole size, the drilling mud resistivity, the effect of invasion of the mud filtrate into the formation, the relation between the recorded thickness of beds and electrode spacing, and the heterogeneity of geologic formations (Archie,
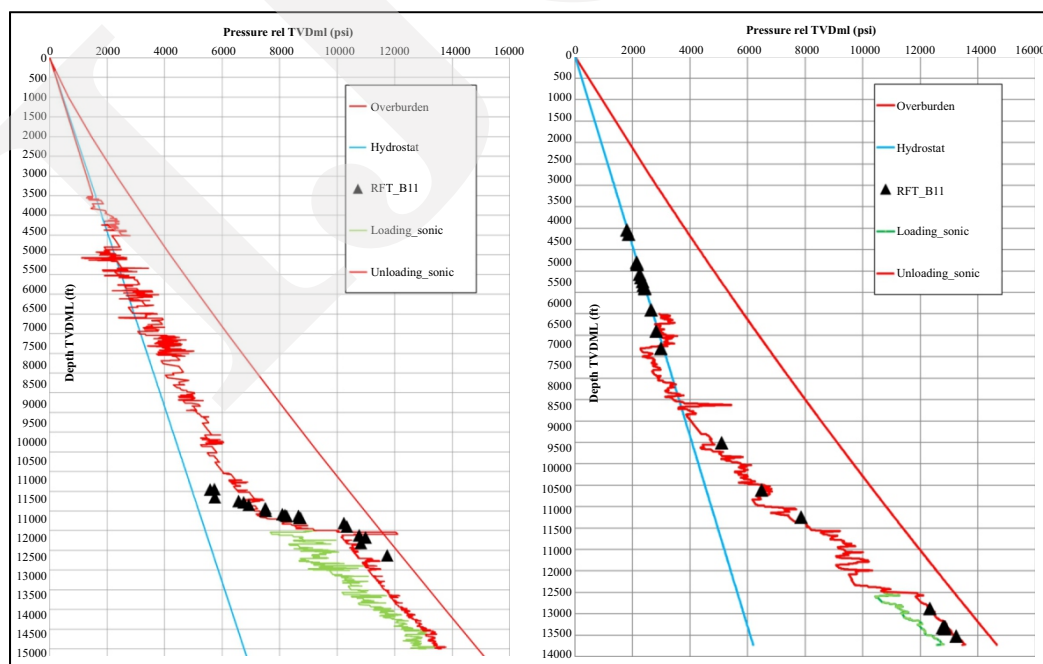

Figure 12. Result of pore pressure estimation in B-11 (left) and SEM-39 (right) using resistivity log.

1942). However, some of these factors also affect the sonic log.

The sonic log has been proven to be effective to interpret pore pressure in the Lower Kutai Basin. This has the advantage of being able to be calibrated with seismic velocities (*e.g.* Reksalegora *et al.*, 2022) in a predictive sense for new drilling. This paper has built on Ramdhan and O'Connor (2022) whereby, even though estimating the total overpressure using an empirical method (*i.e.* Eaton, 1975) is still possible. The method can not differentiate between loading and unloading directly, except by changing the empirical exponent. The repeatable and deterministic approach discussed in this paper uniquely points out the loading contribution to total overpressure.

Based primarily on analyses by Hermanrud *et al.* (1998) from normally and overpressured shales in Norway, the resistivity log is observed to respond in a similar manner to unloading as the sonic log. Figure 11 shows the results of cross-plotting resistivity and vertical effective stress for cooler shales define a concave trend, in contrast to the typical convex shape observed when using sonic data and as recorded in Bowers (1995). This anomalous shape to the resistivity-vertical effective stress trend is seen in similar data from Gulf of Mexico (Hauser *et al.*, 2013), where void ratio, estimated from bulk density, against vertical effective stress, compressional velocity against vertical effective stress, and temperature normalized resistivity against vertical effective stress are displayed. Whilst none of the Gulf of Mexico data displays any data that could be interpreted as unloaded, the similarity with the cooler data in the Lower Kutai Basin adds confidence that the physical characteristics of the rocks are being represented, *i.e.* their rock properties.

Hauser *et al.* (2013) state that resistivity plot vs. vertical effective stress displays a much flatter response to stress over the entire range represented in the data set, resulting in resistivity-based pressure estimates extrapolating in a much more stable manner to higher vertical effective stress. The authors also describe velocity and provide a more stable pressure estimate for a low vertical effective stress. In simple terms, these and our interpretations are that using the resistivity data is less sensitive at a low effective stress, meaning that any pore pressure interpretation will be more inherently uncertain, although as demonstrated in this paper, still potentially useful in a basin where sonic logs (e.g. Rosid *et al.*, 2021) are often missing/not available or run over limited intervals. Conversely, at a high effective stress, the pore pressure given is more accurate than using a sonic log.

With respect to resistivity logs, there is a significant number of resistivity logs in the Lower Kutai Basin (and in other Tertiary basins in Indonesia), and it is apparent that resistivity in the shallower lithologies is affected by freshwater encroachment. An example is seen in Figure 9 from the SEM-39 well, where the resistivity values are high, before loading and unloading are observed. This means that defining a compaction model for this shallow zone and the use of the resistivity log to locate top of overpressure is problematic. A similar thing was reported by Farizi *et al.* (2017) where lateral distribution of apparent water salinity (pure shale and aquifer) along the Tunu Field is mapped, with the salinity increasing from the west to the east, from terrestrial area into the sea environment. This is in line with the regional deposition direction with progradation and salinity increasing seaward, from 10 kppm in delta plain to around 30 kppm in pro-delta. The implication for this paper is that resistivity can be a useful tool to interpret unloaded shales, but care is required in picking representative shale resistivity for the loading model, or focus should be placed on those wells where this encroachment is less significant, *i.e.* B11 in Figure 8.

CONCLUSIONS

The main findings of this paper are:
1. Overpressure-generating mechanisms, as well as their quantification, can be determined more precisely using the deterministic

approach used in this paper. It combines Bowers' (1995) and Dutta's (2002) linear relationship of density and sonic, and this approach is repeatable in other wells from the Lower Kutai Basin.

2. The plausible geological mechanism that contributes to unloading overpressure in the Lower Kutai Basin is gas generation, as reported by Ramdhan and Goulty (2018). This is not explored further in this paper.

3. As an alternative to using the sonic log, analyses by Hermanrud *et al*. (1998) from Norway suggest that the resistivity log reacts in a similar manner to sonic in unloaded shale, and as such, could be a useful new tool in the Lower Kutai Basin for interpretation of pore pressure.

4. Cross-plotting of resistivity vs. vertical effective stress indicates a concave rather than convex trend as displayed in Bowers (1995) for sonic data. This is consistent with observations in Hauser *et al*. (2013) using Gulf of Mexico data.

5. Shallow freshwater encroachment is reported in the Lower Kutai Basin, meaning the shallow resistivity data is problematic to use to define both top of overpressure and a normal compaction trend. Care must therefore be taken if resistivity is to be used for the interpretation of unloaded pore pressure, and to use those wells where this is less pronounced. Regional published salinity studies suggest this would be in the pro-delta area.

6. Assuming the usual caveats in using resistivity data, and the previous point, this paper suggests that resistivity can be a useful tool in the Lower Kutai Basin for pore pressure in unloaded shale at elevated temperatures. This is of relevance in this basin, where sonic logs are either missing or only run over limited intervals.

References

Apranda, Y.R., Riadi, R.S., Nugraha, T., Permana, R.C., and Noeradi, D., 2019. New evaluation on hard overpressure play in Lower Kutai Basin. *Proceedings of the 43rd Annual Convention of the Indonesian Petroleum Association, Indonesia, Jakarta*.

Archie, G.E., 1942. The electrical resistivity log as an aid in determining some reservoir characteristics. *Petroleum Technology,* 5, p.54-62. DOI: 10.2118/942054-G.

Bates, J.A. 1996. Overpressuring in the Kutai Basin: distribution, origins, and implications for the petroleum system. *Proceedings of the 25th Annual Convention of the Indonesian Petroleum Association, Indonesia, Jakarta*.

Bjørkum, P.A. and Nadeau, P.H., 1998. Temperature controlled porosity/permeability reduction, fluid migration, and petroleum exploration in sedimentary basins. *The APPEA Journal,* 38, p.453-465. DOI: 10.1071/AJ97022.

Bois, M., Grosjean, Y., and de Pazzis, L., 1994. Shale compaction and abnormal pressure evaluation application to the offshore Mahakam. *Proceedings of the 23rd Annual Convention of the Indonesian Petroleum Association, Indonesia, Jakarta*.

Bowers, G.L., 1995. Pore pressure estimation from velocity data: accounting for overpressure mechanisms besides undercompaction. *SPE Drilling and Completion*, paper IADC/SPE 27488, 10, p.89-95. DOI: 10.2118/27488-PA.

Bowers, G.L., 2001. Determining an appropriate pore-pressure estimation strategy. *Offshore Technology Conference, Houston, Texas, paper OTC 13042*. DOI: 10.4043/13042-MS

Bowers, G.L., 2002. Detecting high overpressure. *The Leading Edge,* 21, p.174-177. DOI:10.1190/1.1452608.

Bowers, G.L. and Katsube, T.J., 2002. The role of shale pore structure on the sensitivity of wireline logs to overpressure. *In*: Huffman, A.R. and Bowers, G.L. (eds.) Pressure Regimes in Sedimentary Basins and their Prediction.

AAPG, Tulsa, Memoirs, 76, p.43-60. DOI: 10.1306/M76870C5.

Burrus, J. 1998. Overpressure models for clastic rocks, their relation to hydrocarbon expulsion: a critical reevaluation. *In*: Law, B.E., Ulmishek, G.F., and Slavin, V.I. (eds.), Abnormal Pressures in Hydrocarbon Environments. *AAPG, Tulsa, Memoir,* 70, p.35-63. DOI: 10.1306/M70615C3

Chambers, J.L.C., Carter, I., Cloke, R., Craig, J., Moss, S.J., and Paterson, D.W., 2004. Thin-skinned and thick-skinned inversion-related thrusting: A structural model for the Kutai Basin, Kalimantan, Indonesia, *In*: McClay, K.R. (ed.), Thrust tectonics and hydrocarbon systems. *AAPG Memoir,* 82, p.614-634.

DeMatharel, M., Lehmann, P., and Oki, T., 1980. Geology of the Bekapai Field. *In*: Halbouty, M.T. (ed.), Giant Oil and Gas Fields of the Decade 1968-1978. *AAPG, Tulsa, Memoir,* 30, p.459-469. DOI: 10.1306/M30410C22.

Dutta, N.C., 2002. Deepwater geohazard prediction using pre-stack inversion of large offset P-wave data and rock model. *The Leading Edge,* 21, p.193-198. DOI: 10.1190/1.1452612.

Eaton, B.A., 1975. The equation for geopressure prediction from well logs, *SPE, Paper No. 5544*, 11pp. DOI: 10.2118/5544-MS.

Farizi, F., Anwar, T., Hidayat, H.K., Saragih, B., Dodiono, and Tampilang, F., 2017. The proof of dual salinity in Tunu Field: A key information for clay diagenesis and regional overpressure study in Mahakam area. *Proceedings of The 41st Annual Convention of the Indonesian Petroleum Association, Indonesia, Jakarta.*

Gardner, G.H.F., Gardner, L.W., and Gregory, A.R., 1974. Formation velocity and density: the diagnostic for stratigraphic traps. *Geophysics,* 39, p.770-780. DOI: 10.1190/1.1440465.

Ginanjar, Muslim, D., Hendarmawan, and Syafri, I., 2015. Characteristic of pore pressure at the sub surface sedimentary rock in deep water part of Kutai Basin, East Kalimantan, Indonesia. *International Journal of Science and Research,* 6, p.2137-2143. DOI: 10.21275/ART20172742.

Hauser, M.R., Petitclerc, T., Braunsdorf N.R., and Winker, C.D., 2013. Pressure prediction implications of a Miocene pressure regression. *The Leading Edge,* 32, p.100-109. DOI: 10.1190/tle32010100.1.

Hermanrud, C., Wensaas, L., Teige, G.M.G., Vik, E., Nordgård Bolås, H.M., and Hansen, S., 1998. Shale porosities from well logs on Haltenbanken (Offshore Mid-Norway) show no influence of overpressuring. *In*: Law, B.E., Ulmishek, G.F., and Slavin, V.I. (eds.), Abnormal Pressures in Hydrocarbon Environments. *AAPG, Tulsa, Memoir,* 70, p.65-87. DOI: 10.1306/M70615C4.

Hottman, C.E. and Johnson, R.K., 1965. Estimation of formation pressures from log-derived shale properties. *Journal of Petroleum Technology,* 17, p.717-722. DOI:10.2118/1110-PA.

Katahara, K., 2006. Overpressure and shale properties: stress unloading or smectite-illite transformation? *76th SEG Annual Meeting, New Orleans, Louisiana*, *Expanded Abstracts*, p.1520-1524. DOI: 10.1190/1.2369809.

Mann, D.M. and Mackenzie, A.S., 1990. Prediction of pore fluid pressure in sedimentary basins. *Marine and Petroleum Geology,* 7, p.55-65. DOI: 10.1016/0264-8172(90)90056-M.

Moss, S.J. and Chambers, J.L.C., 1999. Depositional modeling and facies architecture of rift and inversion episodes in the Kutai Basin, Kalimantan, Indonesia. *Proceedings of the 27th Annual Convention of the Indonesian Petroleum Association, Indonesia, Jakarta.*

Nysæther, E., 2006. Determination of overpressures in sandstones by fluid flow modelling: the Haltenbanken area, Norway. *Norwegian Journal of Geology,* 86, p.1-27.

Ramdhan, A.M. and Goulty, N.R., 2010. Overpressure-generating mechanisms in the Peciko Field, Lower Kutai Basin, Indonesia. *Petroleum Geoscience,* 16, p.367-376. DOI: 10.1144/1354-079309-027.

Ramdhan, A.M. and Goulty, N.R., 2011. Overpressure and mudrock compaction in The Lower Kutai Basin, Indonesia: A radical

reappraisal. *AAPG Bulletin.* 95, p.1725-1744. DOI: 10.1306/02221110094.

Ramdhan, A.M. Goulty, N.R., and Hutasoit, L.M., 2011. The challenge of pore pressure prediction in Indonesia's warm neogene basins. *Proceedings of the 35th Annual Convention of the Indonesian Petroleum Association, Indonesia, Jakarta*.

Ramdhan, A.M. and Goulty, N.R., 2014. Overpressure in the shelfal area of The Lower Kutai Basin. *Proceedings of the 38th Annual Convention of the Indonesian Petroleum Association, Indonesia, Jakarta*.

Ramdhan, A.M. and Goulty, N.R., 2018. Two-step wireline log analysis of overpressure in the Bekapai Field, Lower Kutai Basin, Indonesia. *Petroleum Geoscience,* 24, p.208-217. DOI: 10.1144/petgeo2017-045.

Ramdhan, A.M. and O'Connor, S.A., 2022. Generation and estimation of overpressure from wireline logs using deterministic approaches in western Indonesia's Tertiary sedimentary basins. *Petroleum Geoscience,* 28. DOI: 10.1144/petgeo2021-062.

Reksalegora, S.W., Hutasoit, L.M., Harsolumakso, A.H., and Ramdhan, A.M., 2022. Pore pressure prediction using velocity-mean effective stress relationship in Madura Sub-basin, East Java Basin - Indonesia. *Indonesian Journal on Geoscience*, 9, p.247-262. DOI: 10.17014/ijog.9.2.247-262

Riadi, R.S., Permana, R.C., Setoputri, A., and Andaryani, S., 2018. Fresh outlook of reservoir understanding and implication for further development strategy of mature fields, case study from Semberah and Mutiara Fields, Kutei Basin, Indonesia. *Proceedings of the 42nd Annual Convention of the Indonesian Petroleum Association, Indonesia, Jakarta*.

Rosid, M.S., Muliandi, Y., and Hafeez, A., 2021. Pore type inversion and s-wave velocity estimation for the characterization of Salawati carbonate reservoir. *Indonesian Journal on Geoscience,* 8, p.131-146. DOI: 10.17014/ijog.8.1.131-146

Teige, G.M.G., Hermanrud, C., Wensaas, L., and Nordgård Bolås, H.M., 1999. The lack of relationship between overpressure and porosity in North Sea and Haltenbanken shales. *Marine and Petroleum Geology,* 16, p.321-335. DOI: 10.1016/S0264-8172(98)00035-X.

Vik, E., Heum, O.R., and Amaliksen, K.G., 1992. Leakage from deep reservoirs: possible mechanisms and relationship to shallow gas in the Haltenbanken area, mid-Norwegian shelf. *In*: England, W.A. and Fleet, A.J. (eds.), Petroleum migration. *Geological Society London, Special Publication* 59*,* 273p. DOI: 10.1144/GSL.SP.1991.059.01.18.

Widyantoro, A. and Santoso, W.D., 2021. Seismic forward modeling of Semberah fluvio-deltaic reservoir. *Proceedings of the 45th Annual Convention of the Indonesian Petroleum Association, Indonesia, Jakarta*.